TECHNICAL NOTE:

STAGNATION-FLOW SOLIDIFICATION ON A FINITE THICKNESS SUBSTRATE

X. Bian and R. H. Rangel [1]

Department of Mechanical and Aerospace Engineering
University of California, Irvine
Irvine, CA 92697 USA

Phone : (714) 824-4033, Fax : (714) 824-8585, e-mail : rhrangel@uci.edu

Accepted for publication in

International Journal of Heat and Mass Transfer

First submission: Aug. 26, 1996

Revised: Feb. 26, 1997

Nomenclature

A	potential-flow strain rate
a_α	α_ℓ/α_s, ratio of the liquid to solid thermal diffusivity
a_k	k_ℓ/k_s, ratio of the liquid to solid thermal conductivity
c	specific heat
h	initial substrate thickness
h_{sf}	latent heat of solidification
k	thermal conductivity
s	solid front position
$\tilde{s}$	dimensionless solid front position ($\tilde{s} = s\sqrt{\frac{A}{\alpha_s}}$)
St	Stefan number ($c(T_m - T_0)/h_{sf}$)
T	temperature

[1] Author to whom correspondence should be addressed.

t	time
v	velocity component of liquid phase in y direction
y	spatial coordinate normal to the substrate
$\tilde{y}$	dimensionless spatial coordinate normal to the substrate ($\tilde{y} = y/\sqrt{\alpha_s/A}$)

Greek symbols

α	thermal diffusivity
η	transformed coordinate
θ	nondimensional temperature $[(T - T_m)/(T_m - T_0)]$
τ	nondimensional time ($\tau = At$)

Subscripts

i	initial
ℓ	liquid phase
o	substrate
m	melting
s	solid phase

Diacritical mark

$\sim$ nondimensional

1. Introduction

Solidification models in which the liquid phase is moving toward the substrate have applications in several important engineering problems such as crystal growth, icing, casting, and others. It is also interesting from a fundamental point of view in metal spray deposition problems, because it allows one to understand the effect of the flow strain on the solidification behavior.

The classical Stefan solidification model considers the solidification of the liquid in a semi-infinite domain in contact with a fixed temperature substrate [1] [2]. The Neumann solution of the Stefan solidification problem has been widely used in the analytical and numerical studies of the droplet deposition process [3] [4] [5] [6]. The stagnation-flow solidification model presented by Rangel and Bian [7] [8] [9] includes the effect of the fluid motion on the solidification process. In these studies, the substrate was represented as a fixed-temperature boundary condition of the solid phase. Another common procedure to include the effect of the substrate on the solidification process is to assume the substrate depth as semi-infinite and the temperature variation of the substrate is solved in this semi-infinite domain [10] [11] [12]. Early experimental and analytical studies of the solidification and melting of a stagnation flow can be found in the work of Savino and Siegel who reported experimental results and analytical studies of the phase change process during the stagnation flow of a warm liquid on a cold plate [13] [14]. In the present work, the effect of the substrate depth on the stagnation-flow solidification problem is studied by analytical and numerical methods. In addition, the effect of the substrate temperature and the liquid temperature and strain rate on the solidification process is investigated. It is shown that the solidification process approaches a quasi-steady behavior, and remelting of the substrate may take place for large substrate depth and higher liquid temperature.

2. Mathematical Formulation

In reference to Fig. 1, consider stagnation flow with an initial temperature T_i impinging on a solid substrate of thickness h and initial temperature T_0. Phase change takes place at the interface and the motion of the interface is controlled by the thermal and fluid dynamics of the problem. The governing equations for this problem are described in [7].

The heat conduction equation for the solid phase is :

$$\frac{\partial^2 T_s}{\partial y^2} = \frac{1}{\alpha_s}\frac{\partial T_s}{\partial t} \qquad \text{in } \; -h < y < s(t),\; t > 0 \tag{1}$$

with the boundary condition: $T_s(y,t) = T_0$ at $y = -h, t > 0$.

Assuming inviscid flow, the energy equation of the liquid phase is

$$\frac{\partial T_\ell}{\partial t} - 2A(y - s(t))\frac{\partial T_\ell}{\partial y} = \alpha_\ell \frac{\partial^2 T_\ell}{\partial y^2} \qquad \text{in} \;\; s(t) < y < \infty, \; t > 0 \tag{2}$$

with the boundary condition: $T_\ell(y,t) \to T_i$ as $y \to \infty$.

The coupling conditions at the interface $y = s(t)$ are:

$$T_s(y,t) = T_\ell(y,t) = T_m \tag{3}$$

$$k_s \frac{\partial T_s}{\partial y} - k_\ell \frac{\partial T_\ell}{\partial y} = \rho h_{sf} \frac{ds(t)}{dt} \tag{4}$$

Remelting of the substrate plays an important role in enhancing the bonding characteristics of the deposit. The occurence of remelting at $t = 0$ may be predicted using the Schwarz solution reported in [1]. The criterion for initial remelting when the liquid initial temperature is T_i and the substrate initial temperature is T_0 is:

$$\frac{T_i - T_m}{T_m - T_0} - \frac{\sqrt{a_\alpha}}{a_k} > 0 \tag{5}$$

3. Quasi-Steady Solution

In analogy to the quasi-steady solution of the inviscid stagnation-flow solidification on a constant temperature cold substrate [7], a quasi-steady solution is used to study the long-time solidification behavior of the problem.

In employing the quasi-steady approximation, we neglect the time derivative in the governing equations (1) and (2). The boundary and initial conditions remain unchanged.

The solid-phase equation has the solution,

$$\theta_s = \frac{T_s - T_m}{T_m - T_0} = \frac{y - s}{h + s} \tag{6}$$

while the liquid-phase solution is,

$$\theta_\ell = \frac{T_\ell - T_m}{T_i - T_m} = \frac{\displaystyle\int_s^y \exp\left[-\tfrac{2A}{\alpha_\ell}\left(\tfrac{y'^2}{2} - sy'\right)\right] dy'}{\displaystyle\int_s^\infty \exp\left[-\tfrac{2A}{\alpha_\ell}\left(\tfrac{y'^2}{2} - sy'\right)\right] dy'} \tag{7}$$

The energy balance [equation (4)] can be written as

$$\rho h_{sf}\frac{ds}{dt}=\frac{k_s(T_m-T_0)}{h+s}-\frac{k_\ell(T_i-T_m)\exp(\frac{As^2}{\alpha_\ell})}{\displaystyle\int_s^\infty \exp\left[-\frac{2A}{\alpha_\ell}\left(\frac{y'^2}{2}-sy'\right)\right]dy'} \tag{8}$$

Employing the error function, equation (8) can be simplified to:

$$\rho h_{sf}\frac{ds}{dt}=\frac{k_s(T_m-T_0)}{h+s}-2(T_m-T_0)\theta_i k_\ell\sqrt{\frac{A}{\pi\alpha_\ell}} \tag{9}$$

which in turn can be rewritten in dimensionless form as

$$\frac{1}{St}\frac{d\tilde{s}}{d\tau}=\frac{1}{\tilde{h}+\tilde{s}}-\frac{2a_k\theta_i}{\sqrt{a\pi}}. \tag{10}$$

The asymptotic value of $\tilde{s}$ can now be obtained by using the fact that $\frac{d\tilde{s}}{d\tau}\to 0$ as $\tau\to\infty$ [7]. Then equation (10) gives

$$\tilde{s}\to-\tilde{h}+\frac{\sqrt{a_\alpha\pi}}{2a_k\theta_i} \qquad as \quad \tau\to\infty \tag{11}$$

which indicates that there exits an upper limit of the solid phase thickness as time goes to infinity. This solution also shows that if $\tilde{h}=\sqrt{a_\alpha\pi}/(2a_k\theta_i)$, the final interface location is equal to the initial one. Furthermore, the final solid thickness is independent of $\tilde{h}$.

4. Finite-difference solution

For the numerical solution, it is convenient to recast the system of equations in dimensionless form as:

$$\frac{\partial\theta_s}{\partial\tau}=\frac{\partial^2\theta_s}{\partial\tilde{y}^2} \qquad \text{for} \quad -\tilde{h}<\tilde{y}<\tilde{s}(\tau) \tag{12}$$

$$\frac{\partial\theta_\ell}{\partial\tau}-2(\tilde{y}-\tilde{s}(\tau))\frac{\partial\theta_\ell}{\partial\tilde{y}}=a_\alpha\frac{\partial^2\theta_\ell}{\partial\tilde{y}^2} \qquad \text{for} \quad \tilde{s}(\tau)<\tilde{y}<\infty \tag{13}$$

$$\theta_\ell=\theta_s \qquad \text{and} \quad \frac{\partial\theta_s}{\partial\tilde{y}}-a_k\frac{\partial\theta_\ell}{\partial\tilde{y}}=\frac{1}{St}\frac{d\tilde{s}}{d\tau} \qquad \text{at} \quad \tilde{y}=\tilde{s}(\tau) \tag{14}$$

Since the solution domains for the solid and liquid phases vary with time because of the moving interface position, the following transformations

$$\eta_s=\frac{4}{\pi}\tan^{-1}\left(\frac{\tilde{y}-\tilde{s}}{\tilde{h}+\tilde{s}}\right) \tag{15}$$

$$\eta_\ell=\frac{2}{\pi}\tan^{-1}(\tilde{y}-\tilde{s}) \tag{16}$$

are applied to transform the solution domain $(-\tilde{h}, \tilde{s})$ into $(-1, 0)$, and $(\tilde{s}, \infty)$ into $(0, 1)$. After the coordinate transformations, the Crank-Nicolson scheme is applied to obtain the finite-difference form of the system of equations. This system can then be solved to obtain the time-variation of the temperature distributions of the solid and liquid phases as well as the interface location. Similar transformations are employed in references [8] and [12].

5. Results and discussion

Finite-difference solutions are obtained to study the stagnation-flow solidification process on a finite-thickness substrate of the same material. Aluminum properties are employed. The effect of strain rate, Stefan number and other transport properties have been reported earlier for the limiting case of zero-thickness substrate at fixed temperature [7]-[9]. Figure 2 shows the effect of substrate thickness on the time evolution of the solid-front location. The most important feature is that the solid-front location approaches a fixed position predicted by the quasi-steady solution. If the initial solid substrate is thick enough, $\tilde{h} = 10$ for example, it can be observed that the liquid will be solidified initially, but as time increases, the substrate will be remelted and the final position of the solid front will be lower than the initial interface. On the other hand, if the initial substrate thickness is sufficiently thin, the behavior of the solid-front location resembles the result obtained for the case of stagnation-flow solidification on a substrate with constant temperature [7] [8]. The case for $\tilde{h} = 9.18$ corresponds to the situation where the final interface location is equal to its initial value.

The effect of the flow strain rate on the solidification behavior can be observed in Fig.3. The strain rate is absorbed into the dimensionless time and position and therefore, in order to see its effect, the solution must be plotted in dimensional units. For the case of aluminum with $T_i = 1033K$, $T_0 = 300K$, $T_m = 933K$, Fig. 3 shows that increasing the strain rate results in a decrease of the height of the final solid-front location. Increasing the strain rate, increases the heat flux to the interface from the liquid side which has an adverse effect on the solidification process.

The dimensionless temperature distribution for two different substrate thicknesses at different times is shown in Fig. 4. It can be observed that in the final stages of solidification, the slope of the temperature distribution at the interface ($\theta = 0$) on the solid side is very different from that in early times. The solid-side temperature gradient decreases, while the liquid-side temperature gradient remains constant due to the fact that the liquid temperature approaches a quasi-steady behavior more rapidly than the solid temperature does.

The effect of the initial liquid and substrate temperature on the solidification process is shown in Fig. 5. It can be seen that increasing the initial temperature of the liquid to a high enough value will result in the remelting of the substrate. Increasing the initial temperature of the substrate will decrease the height of the final solid phase thickness. For a sufficiently thick substrate, the final solid front will be located below the original interface.

Acknowledgement

This work has been supported by a grant from the National Science Foundation (CTS-9224856).

References

[1] H. S. Carslaw and J. C. Jaeger, *Conduction of Heat in Solids* , 2nd ed., p. 283, Clarendon Press, London, 1959.

[2] M. N. Ozisik, *Heat Conduction* , 1st ed., p. 439, John Wiley & Sons, New York, 1980.

[3] J. Madejski, Solidification of Droplets on a Cold Surface, *Int. J. Heat Mass Transfer*, **19**, 1009-1013 (1976).

[4] J. Madejski, Droplets on Impact with a Solid Surface, *Int. J. Heat Mass Transfer*, **7**, 1095-1098 (1983).

[5] H. Liu, E. J. Lavernia and R. H. Rangel, Numerical Simulation of Substrate Impact and Freezing of Droplets in Plasma Spray Processes, *J. Phys. D: Appl. Phys.*, **26**, 1900-1908 (1993).

[6] C. San Marchi, H. Liu, E. J. Lavernia and R. H. Rangel, Numerical Analysis of the Deformation and Solidification of a Single Droplet Impinging onto a Flat Substrate, *J. of Materials Sc.* **28**, 3313-3321 (1993).

[7] R. H. Rangel and X. Bian, The Inviscid Stagnation-flow Solidification Problem, *Int. J. Heat Mass Transfer*, **39**, 1591-1602 (1996).

[8] R. H. Rangel and X. Bian, Numerical Solution of the Inviscid Stagnation-Flow Solidification Problem, *Numerical Heat Transfer-Part A*, **28**, 589-603 (1995).

[9] X. Bian and R. H. Rangel, The Viscous Stagnation-Flow Solidification Problem, *Int. J. Heat Mass Transfer*, **39**, 3581-3594 (1996).

[10] C. H. Amon, K. S. Schmaltz, Numerical and Experimental Investigation of Interface Bonding via Substrate Remelting of an Impinging Molten Metal Droplet. *J. Heat Transfer-Transactions of the ASME*, **118**, 164-172 (1996).

[11] B. Kang, J. Waldvogel, D. Poulikakos, Remelting Phenomena in the Process of Splat Solidification, *J. of Materials Sc.* **30**, 4912-4925 (1995).

[12] R. H. Rangel and X. Bian, Metal-Droplet Deposition Model Including Liquid Deformation and Substrate Remelting, *Int. J. Heat Mass Transfer*, in press (1997).

[13] J. M. Savino and R. Siegel, Experimental and Analytical Study of the Transient Solidification of a Warm Liquid Flowing over a Chilled Flat Plate. *NASA-TN D-4015* (1967).

[14] J. M. Savino and R. Siegel, An Analytical Solution for Solidification of a Moving Liquid onto an Isothermal Cold Wall. *Int. J. Heat Mass Transfer*, **12**, 803-809 (1969).

Figure Captions

Fig. 1. Solidification in a half space: the stagnation flow solidification on a finite thickness substrate.

Fig. 2. Effect of substrate thickness ($T_0 = 300K, T_i = 1033K, a_\alpha = 0.43, a_k = 0.40, St = 1.67$).

Fig. 3. Solid-front time evolution for different strain rates ($T_0 = 300K, T_i = 1033K, h = 0.1mm$).

Fig. 4. Effect of the substrate thickness on the temperature distribution ($T_0 = 300K, T_i = 1033K$).

Fig. 5. Effect of initial liquid and substrate temperatures on the solid-front time evolution ($\tilde{h} = 1$).

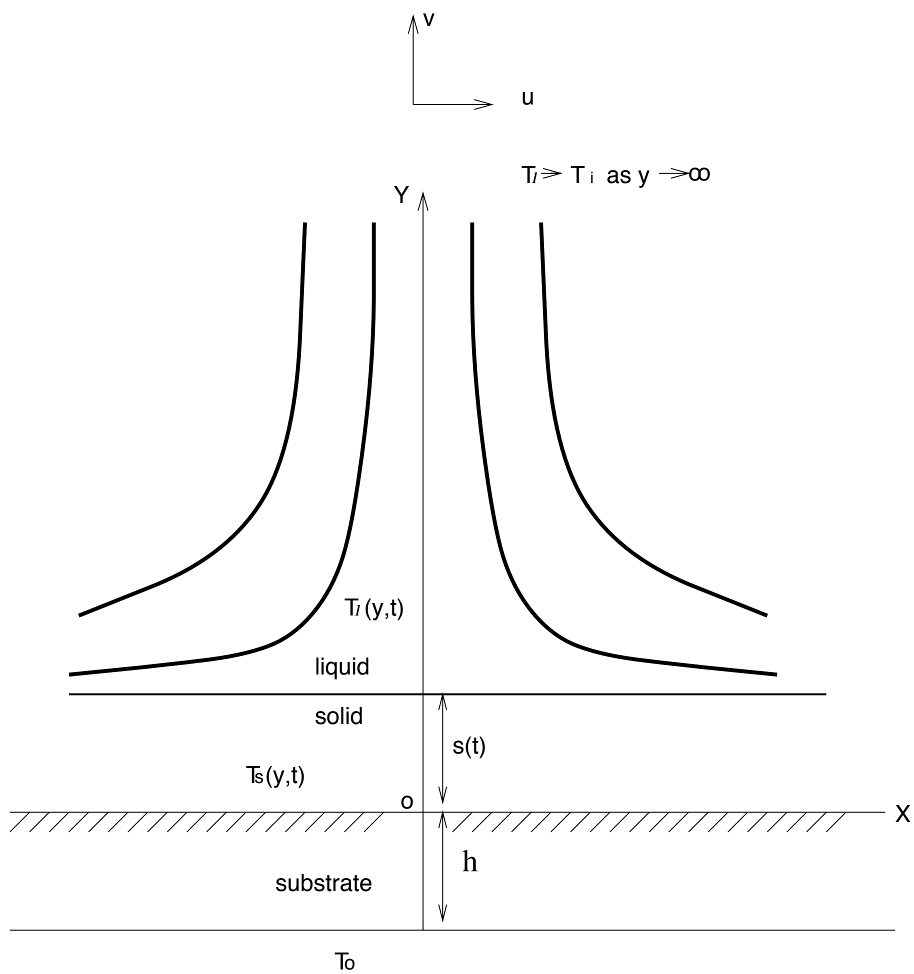

Fig. 1 Bian and Rangel

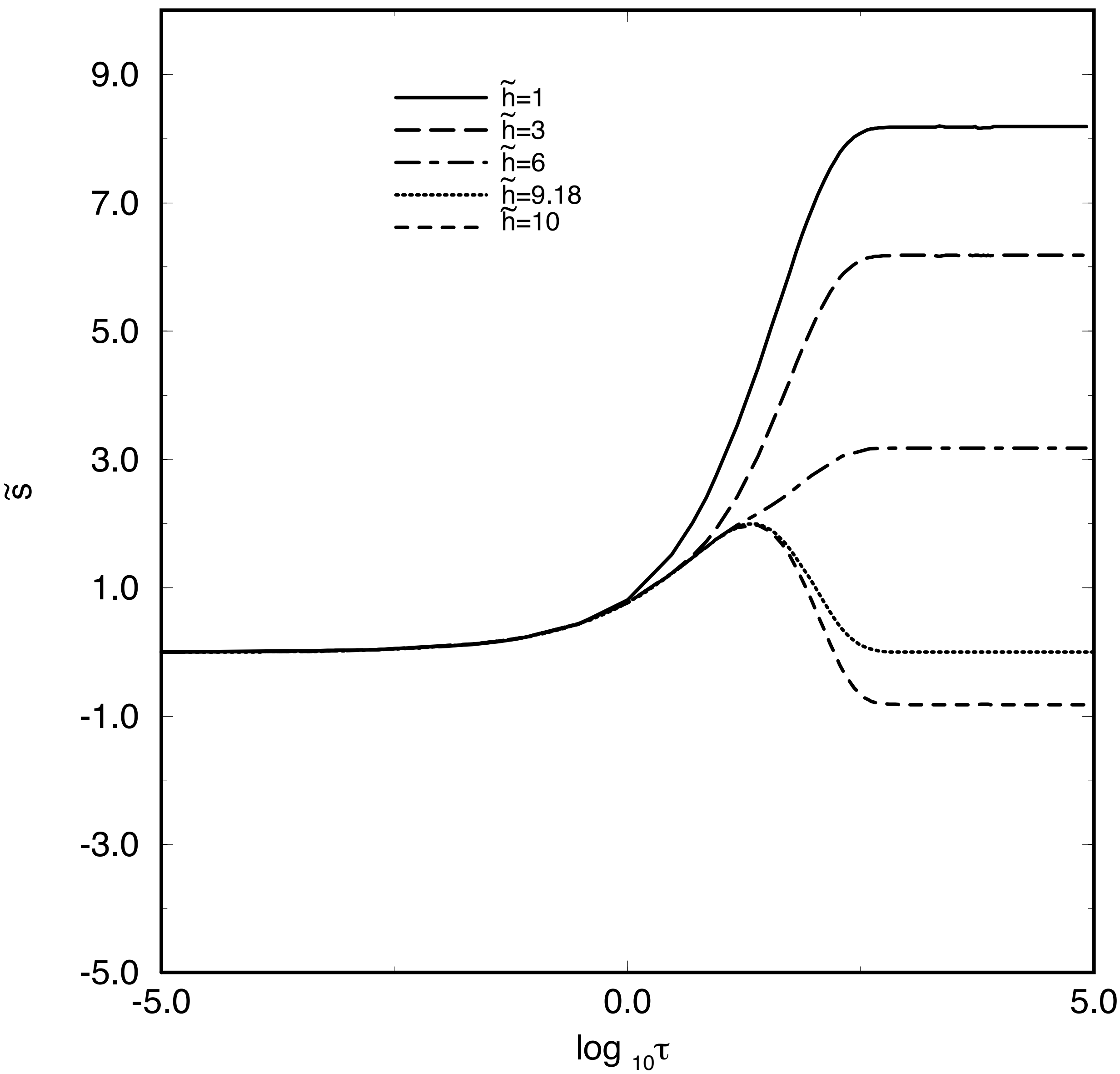

Fig. 2 Bian and Rangel

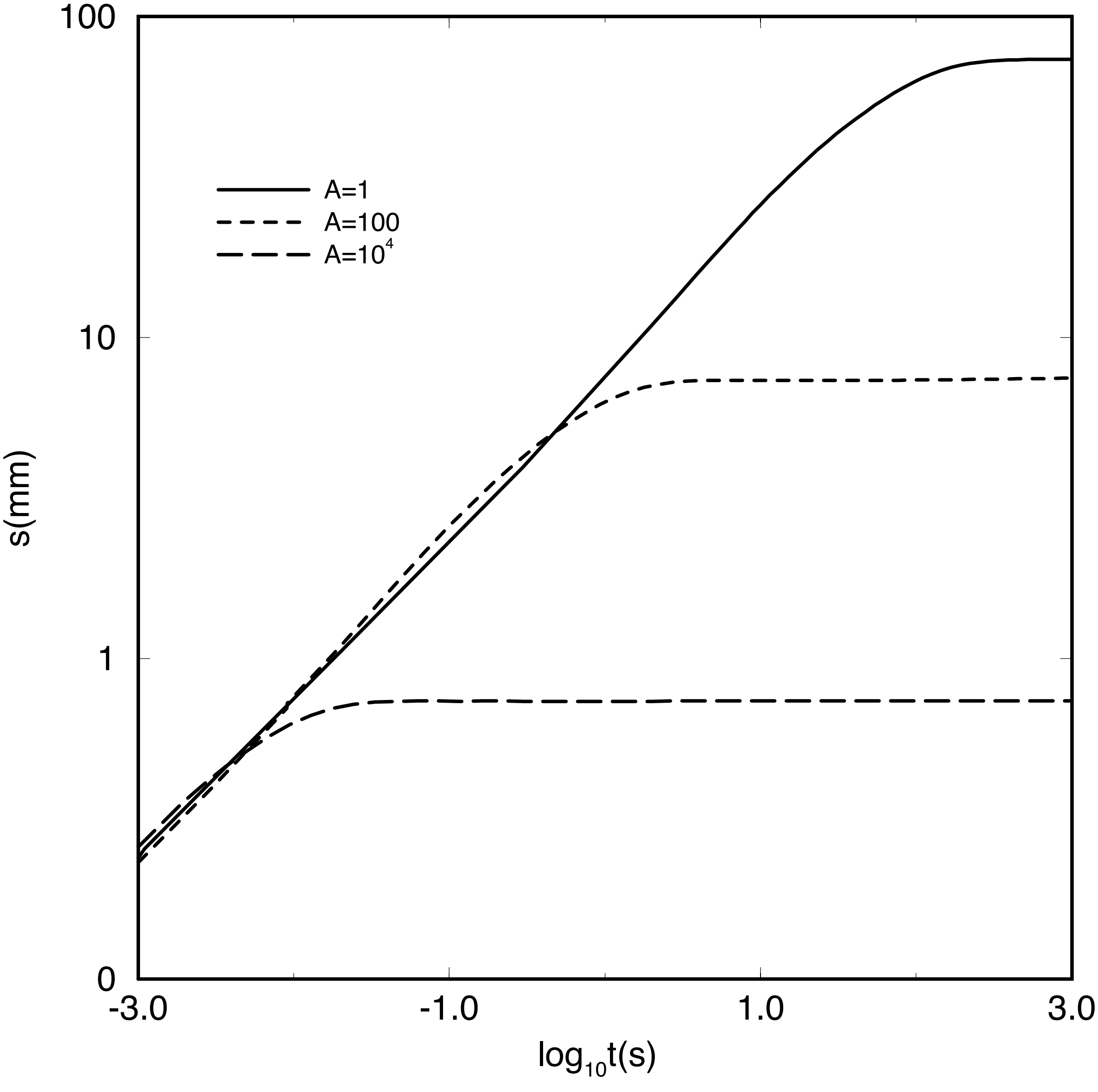

Fig. 3 Bian and Rangel

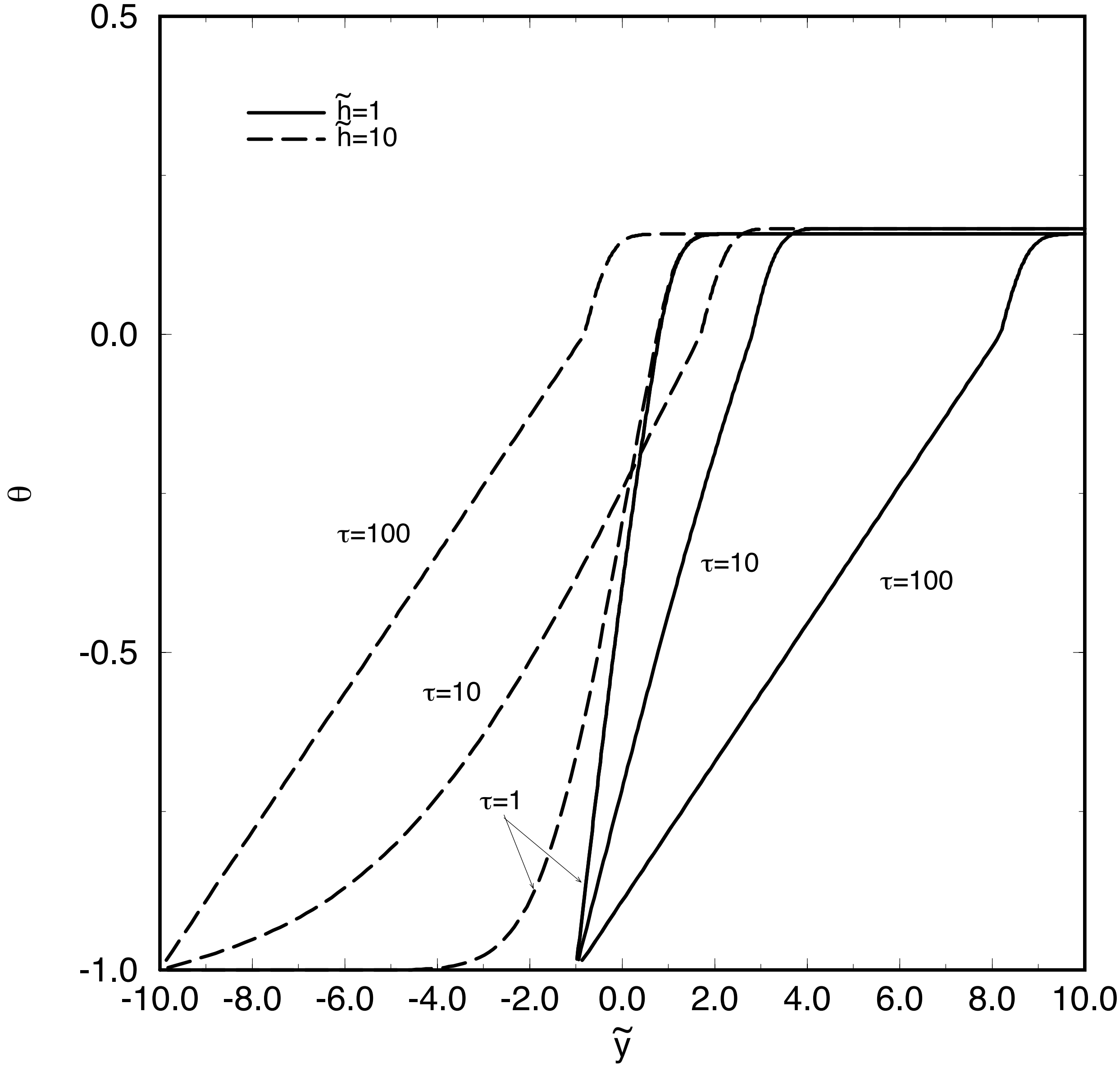

Fig. 4 Bian and Rangel

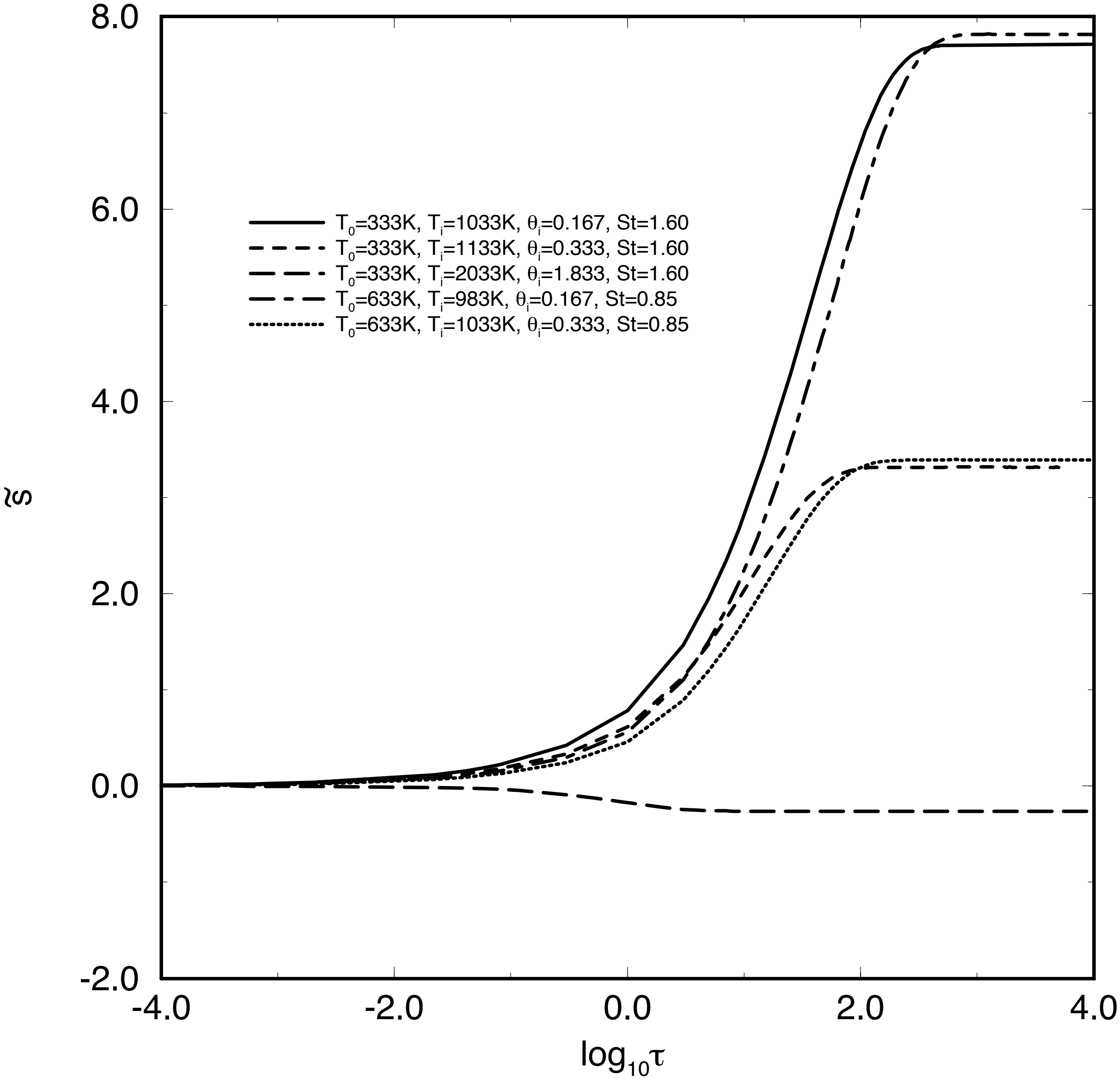

Fig. 5 Bian and Rangel